Mass Spectrometry
DOI: 10.5702/massspectrometry.A0124

Vol. 12 (2023), A0124

Original Article

Identification of Negative Ion at *m/z* 20 Produced by Atmospheric Pressure Corona Discharge Ionization under Ambient Air

Shiho Fujishima, Kanako Sekimoto, and Mitsuo Takayama*

Graduate School in Nanobioscience, Yokohama City University, 22–2 Seto, Kanazawa-ku, Yokohama 236–0027, Japan

The negative ion at *m/z* 20 observed at atmospheric pressure corona discharge ionization mass spectra has been identified by supplying the vapors of deuterium oxide (D_2O) and $H_2{}^{18}O$. From the mass shifts of the ion at *m/z* 20 observed with D_2O and $H_2{}^{18}O$, it was suggested that the chemical composition of the ion at *m/z* 20 is to be H_4O. Further mass shift from *m/z* 20 to 22 was observed by supplying the vapor of perfluorokerocene, suggesting the chemical composition of H_3F. The chemical compositions of the negative ions H_4O^- and H_3F^- were consistence with the dipole-bound complex states between hydrogen H_2 and polar molecules such as H_2O and hydrogen fluoride (HF) having dipole moments beyond a critical dipole moment of 1.625 D, theoretically proposed by Skurski and Simons. The ionic chemical compositions and structures of H_4O^- and H_3F^- obtained with density functional theory calculations implied that both dipole-bound complex $H_2O^-\ldots H_2$ and $HF^-\ldots H_2$ can be formed by exothermic reactions by which H_2 molecule is complexing with negative ions H_2O^- and HF^-, respectively.

Please cite this article as: Mass Spectrom (Tokyo) 2023; 12(1): A0124

Keywords: negative ion at *m/z* 20, corona discharge, hydrogenated water cluster H_4O^-, dipole-bound complex, density functional theory

(Received: January 12, 2023; Accepted: May 23, 2023; advance publication released online June 21, 2023)

1. INTRODUCTION

We and Nagato *et al*. have previously reported that atmospheric pressure corona discharge ionization (APCDI) of ambient air resulted in various kinds of negative ions Y^- ($Y=CO_x$, HCO_x, NO_x, HNO_x, O_x, HO_x) and water clusters $Y^-(H_2O)_n$.[1–4] Although almost negative ions generated by APCDI have been identified, a small mass ion at *m/z* 20 remains unknown to date.[3] The negative ion at *m/z* 20 can be observed at high voltage conditions such as −2.7 and −3.5 kV applied to the corona needle, while at low voltage conditions such as −1.9 kV, the hydroxide HO^- and its water clusters $HO^-(H_2O)_n$ can be observed by accompanying a magic cluster of $HO^-(H_2O)_3$ at *m/z* 71.[2,3] The hydroxide HO^- can be formed by an ion molecule reaction between O^- and H_2O[1,5] or by the attachment of electron to hydroxyl radicals ·OH due to its positive electron affinity (EA, 1.83 eV),[6] while it is believed that the hydroxyl radicals ·OH are generated *via* dissociation of water molecules on the tip of needle. The dissociation of water molecules into hydroxyl and hydrogen radicals (·OH + H·) may occur on the tip with high electric field strength such as 10^8–10^9 V/m resulting in over 100 eV kinetic energy of electrons.[3,7] Regarding the dissociation of water molecules on the steel surface, Takahashi *et al*. showed that water molecules attached to the steel surface heated easily dissociate into ·OH and H· radicals.[8] From this, it is expected that some kind of negative ions originated from hydrogen radical H· and/or hydride H^- can be observed, because the hydrogen radical has a positive value of EA 0.75 eV.[6]

Here we identify the negative ion at *m/z* 20 as a dipole-bound complex ion H_4O^- between hydrogen, water, and electron, proposed by Skurski and Simons.[9] Another negative ion at *m/z* 22 corresponding to H_3F^- produced by supplying hydrogen fluoride (HF) gas is also identified as the dipole-bound complex. The stability and structures of H_4O^- and H_3F^- are discussed from the point of quantum chemical calculations.

2. EXPERIMENTAL

2.1. APCDI mass spectrometry

All the mass spectra were obtained with a reversed geometry double-focusing mass spectrometer JMS-BU30 (JEOL, Tokyo, Japan) attached to a home-build ion source of APCDI. The schematic illustration and main experimental conditions have been reported elsewhere.[2,3] The discharge gap *d*

*Correspondence to: Mitsuo Takayama, *Graduate School in Nanobioscience, Yokohama City University, 22–2 Seto, Kanazawa-ku, Yokohama 236–0027, Japan*, e-mail: takayama@yokohama-cu.ac.jp

between the electrodes and the needle angle α with respect to the orifice axis were adjusted to 3 mm and 0 rad, respectively. An angle of 0 rad is defined as the needle being located on the orifice axis. The needle was located perpendicular to the orifice plate as a plane electrode and could be shifted parallel of 0 and 1 mm to the orifice plate. The DC voltage of −2.0 kV was applied to the needle relative to the orifice plate. It is of importance to recognize that the conditions of the angle at 0 rad and the center location at 0 mm of the needle give high electric field strength even at the DC voltage of −2.0 kV.[2,3,7] The orifice was heated at 40°C to generate hydrated clusters $Y^-(H_2O)_n$. The room temperature of 298 K and relative humidity of 30–68% were controlled by a standard commercial air conditioner. For evaluating the correlations between the ion at *m/z* 20 and the negative ions at *m/z* 16 (O^-) and *m/z* 33 (HO_2^-), the DC voltage of −2.0 to −3.4 kV and the needle location of 1 mm were employed under room temperature and 54% humidity. HF gas was generated by using a home-build reaction system made up of ultraviolet light, polytetrafluoroethylene (PTFE), and hydrogen gas.[10] Using the system, the HF gas was generated by which fluorine was abstracted by hydrogen radicals from the surface of PTFE due to the difference of bond dissociation energy for HF and carbon–fluorine (CF) bonds.

2.2. Reagents

Perfluorokerocene (PFK, low boiling) was purchased from Tokyo Chemical Industry (Tokyo, Japan). D_2O (99.9 atom%) and heavy oxygen water ($H_2{}^{18}O$, 99 atom%) were purchased from Sigma-Aldrich (St. Louis, MO, USA).

2.3. Calculations

All the calculations reported in this paper have been performed using the Gaussian 16 suite of programs,[11] and the initial molecules and ionic structures of non-covalent complex ions $(H_2…H_2O)^-$ and $(H_2…HF)^-$ were generated by means of visual inspection using the GaussView program 6.0.[11] The geometry optimization and vibration frequency analysis of all mentioned species were performed with the M06-2X hybrid functional[12] level of theory and 6-31G+(d,p) basis set.

3. RESULTS AND DISCUSSION

3.1. Conditions for observing the definite ion peak at *m/z* 20

Figure 1 shows negative ion APCDI mass spectra of ambient air obtained with three different humidity conditions, at low electric field strength. The spectra obtained at 50 and 68% in humidity showed ion peaks at *m/z* 20 and/or 38, as well as the peaks corresponding to hydroxide HO^- at *m/z* 17 and its water clusters $OH^-(H_2O)_n$ (*n*=1–4) at *m/z* 35, 53, 71, and 89, while the humidity 30% did not result in the ion at *m/z* 20. Figure 2 shows the spectra obtained at high electric field strength, under three different humidity conditions. As already reported,[3] the high electric field resulted in various kinds of marked negative ions such as O^-, HCN^-, CO^-, HCO^-, HO_2^-, N_2O^-, NO_2^-, NO_3^-, HNO_3^-, and $NO_2^-(NO_2)$ as shown in Fig. 2. Interestingly, the spectra with high electric field strength showed the definite ion at *m/z* 20 together with its water clusters at *m/z* 38, 56, and 74 (Fig. 2C). The results obtained above indicate that the conditions of high humidity and high electric field strength are favorable for the formation of the negative ion at *m/z* 20. Especially, the influence of the high humidity in Figs. 1C and 2C suggests that the negative ion at *m/z* 20 might be composed from a water molecule H_2O, and this means that the ion is made up of H_2O and H_2.

As was reported in the previous paper,[3] the ion at *m/z* 20 could be observed under relatively high electric field conditions. This may be due to that the high electric field results in efficient ionization of O_2, abundant dissociation of O_2^- and H_2O, and the sequential progress of the ion-molecule reactions.[2–4] Especially, the negative ions of O^-, HO^-, and HO_2^-, and radical species such as $HO_2\cdot$ and $HO\cdot$ are generated by higher kinetic energy of electrons.[4] At the same time, the hydrogen radical H· and/or hydride H^- may be generated from water molecules by the high kinetic energy electrons and/or by the dissociation of water molecules on the tip of the needle, although the H· and H^- could not be detected by the mass spectrometer used. As a result, it is considered that the ion at *m/z* 20 is generated by which water molecules interact with H· and/or H^-. Here we show the data of positive correlation of the formation of the ion at *m/z* 20 with the formation of the ions corresponding to O^- at *m/z* 16 and HO_2^- at *m/z* 33 (Fig. 3). The correlations showed in Fig. 3 were made from the numerical data (Table 1) obtained with the DC voltage of −2.0 to −3.4 kV and the needle location of 1 mm. These correlations indicate that the high electric field conditions are favorable for the formation of H_4O^-, O^-, and HO_2^- ions, although the involvement of atomic hydrogens is not clear.

3.2. Influence of the vapor of D_2O and $H_2{}^{18}O$ on the mass shift of the ion at *m/z* 20

To examine the favorable conditions for appearance of the ion at *m/z* 20, the influence of the vapor of water on the spectral patterns was studied by using D_2O and $H_2{}^{18}O$. The application of the high humidity condition at 68% resulted in the definite peaks at *m/z* 20, 38, 56, and 74 (Fig. 2C), while lower humidity at 30% did not result in such ion peaks (Fig. 2A). This suggests that the ion at *m/z* 20 and its water clusters $20^-(H_2O)_n$ (*n* = 1–3) are expedited by supplying the vapor of water. Therefore, it is expected that the mass shift of the ion at *m/z* 20 would be observed *via* the H/D or $^{16}O/^{18}O$ exchange by supplying the vapor of D_2O or $H_2{}^{18}O$. To confirm the influence of the water molecules on the mass shift of the ion at *m/z* 20, the vapors of D_2O and $H_2{}^{18}O$ were supplied into the region of corona discharge under the conditions of high electric field strength, room temperature, and 57% humidity. The spectra obtained with supplying the vapor of D_2O showed the mass shift *n* at *m/z* *m* + *n* (*m* = 20, 38, 56), *i.e.*, *n* = 1–4 for *m/z* 20, *n* = 1–4 for *m/z* 38, and *n* = 1–2 for *m/z* 56, as shown in Fig. 4. The mass shift *n* at *m/z* 20 + *n* (*n*=1–4) indicates that the H/D exchange to form the ions at *m/z* 21 (= 20 − H + D), *m/z* 22 (= 20 − 2H + 2D), *m/z* 23 (= 20 − 3H + 3D), and *m/z* 24 (20 − 4H + 4D) takes place by supplying the vapor of D_2O. This suggests that unknown species of the ion at *m/z* 20 has a composition of 16 + 4H.

To obtain further information about the chemical composition of the ionic species at *m/z* 20, the vapor of $H_2{}^{18}O$ was supplied in expectation of the mass shift by the $^{16}O/^{18}O$ exchange. The resulting spectra showed the peaks at *m/z* 19, 22, 30, 37, and 40, as shown in Fig. 5. The ion at *m/z* 19 represents $H^{18}O^-$ ion produced by the $^{16}O/^{18}O$ exchange of HO^- ion at *m/z* 17. The ion at *m/z* 22 may be corresponding to the *m/z* 22 (=20 − ^{16}O + ^{18}O). From the results obtained by the experiments with D_2O and $H_2{}^{18}O$ described above, it is strongly suggested that the

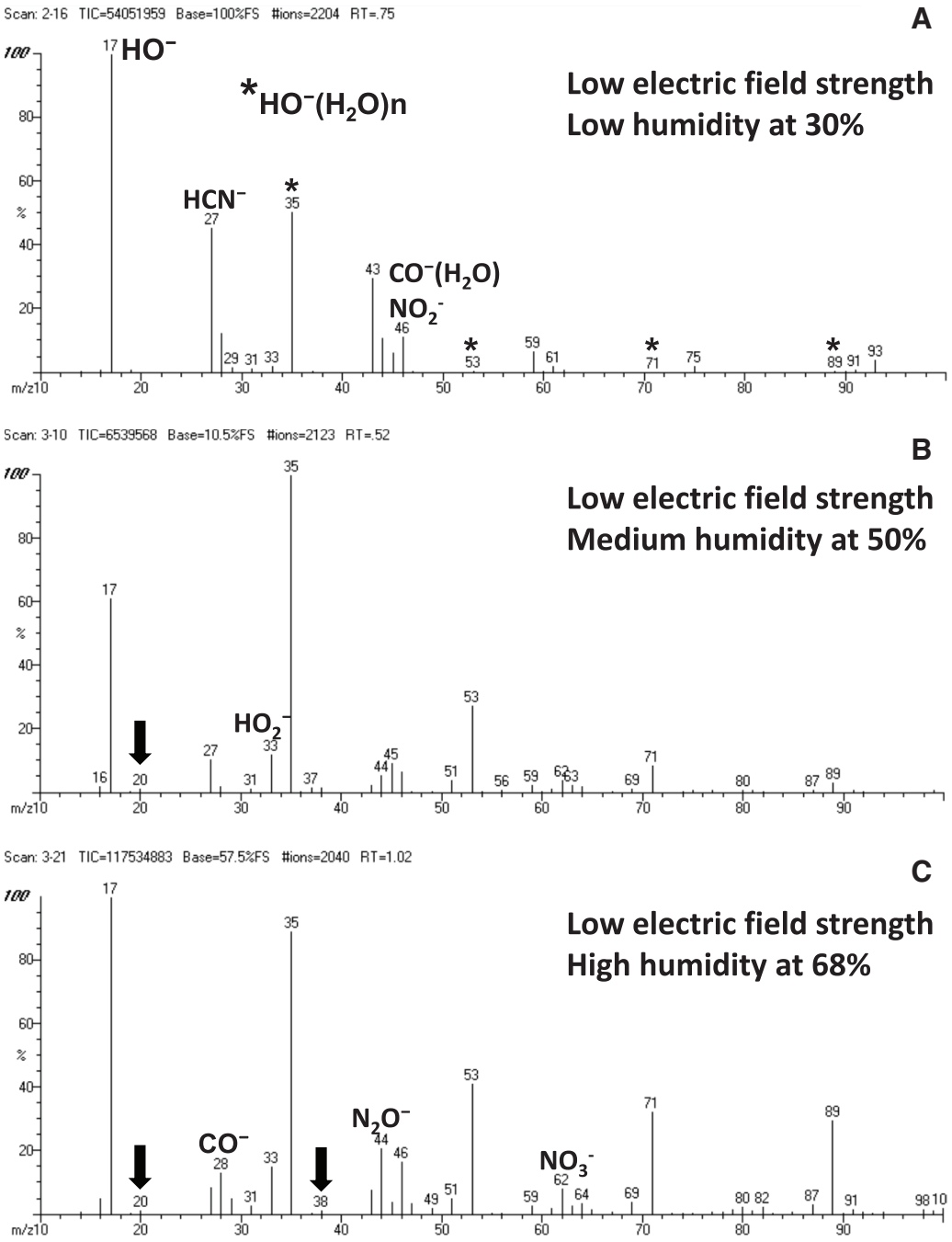

Fig. 1. Negative-ion APCDI mass spectra of ambient air obtained with the low electric field strength at −2.0 kV and needle position of 1 mm under room temperature and three different humidity of (A) 30%, (B) 50%, and (C) 68%. APCDI, atmospheric pressure corona discharge ionization.

chemical composition of the ion at *m/z* 20 has H_4O, although this is an unusual chemical composition.

The results obtained above suggest that the ion at *m/z* 20 has ionic chemical compositions of $H_2^-(H_2O)$, $H_2(H_2O^-)$, $H^-(H_3O)$, and $HO^-(H_3)$ or an electron delocalized composition H_4O^-. Although the values of EA of H_2, H_2O, H, and HO are all positive, *i.e.*, 0.9 eV,[13] 1.3 eV,[14] 0.75 eV,[6] and 1.83 eV,[6] respectively, it is known that the negative ion H_2^- has short lifetimes 8–11 μs and rapidly dissociates into H^- and H·.[15] The ion at *m/z* 20 observed in Figs. 1 and 2 was measured through the length of 3 mm under ambient air and the flight length of *ca.*1000 mm in a double-focusing mass spectrometer. This indicates that the ionic chemical composition of $H_2^-(H_2O)$ consisted of H_2^- as the core ion would be deleted from the candidates described above. Regarding the unusual chemical composition H_4O of the negative ion at *m/z* 20 formed of hydrogen and water molecules, there is an interesting report that unusual molecular anions in their dipole-bound ground state are produced *via* charge exchange between polar molecules and high Rydberg atoms.[16] A possibility has been shown that such dipole-bound anions made of polar molecules beyond a critical dipole moment of 1.625 D will form bound anion states.[17] Indeed, some polar molecules such as H_2O and HF have dipole moments of 1.857 and 1.827 D, respectively.[18] Skurski *et al.* have reported that using a theoretical concept of molecular trap, unstable or metastable anions such as N_2^- and H_2^- can be stabilized by trapping with polar molecules,[9,19] although it is unclear whether the

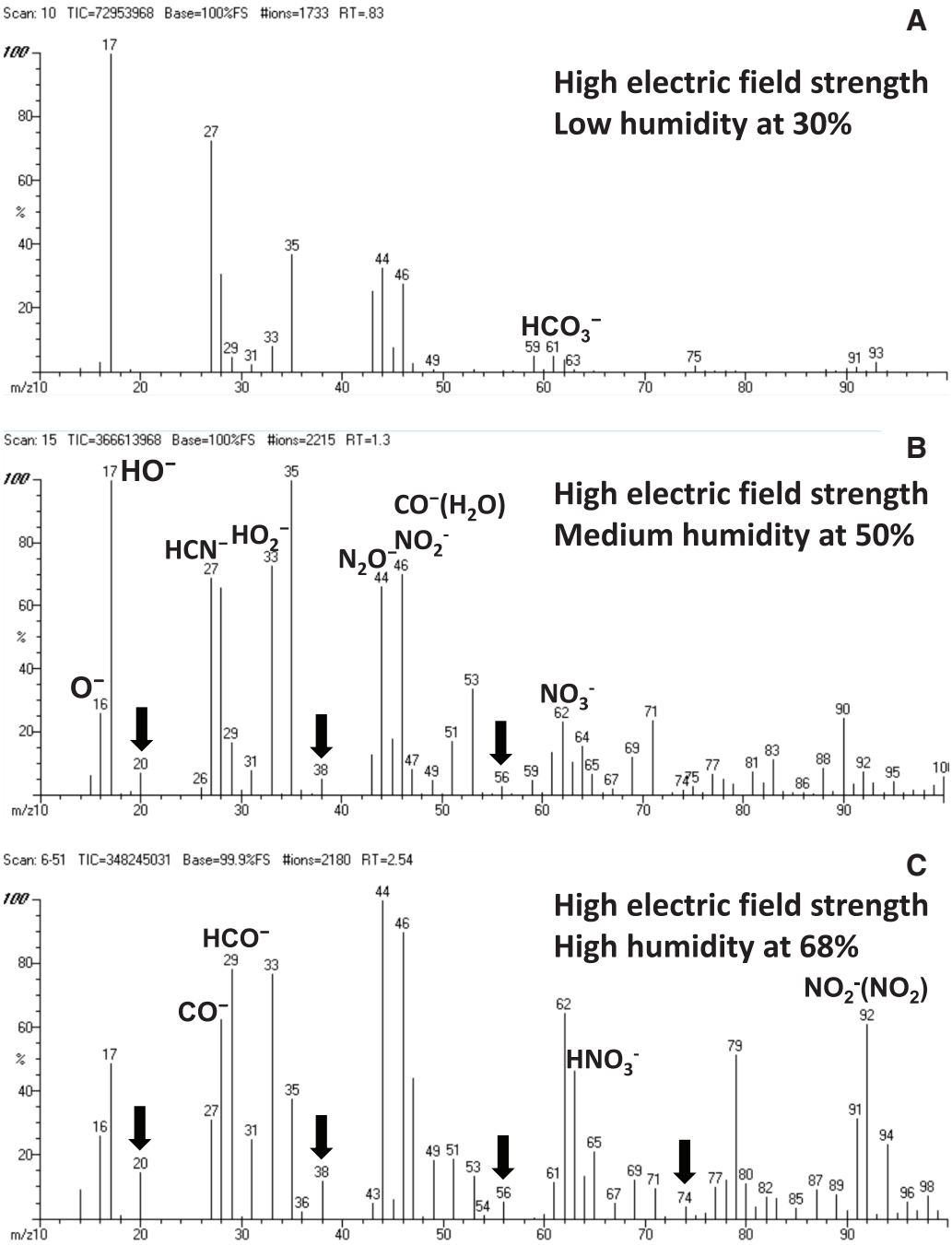

Fig. 2. Negative-ion APCDI mass spectra of ambient air obtained with the high electric field strength at −2.0 kV and needle position of 0 mm under room temperature and three different humidity of (A) 30%, (B) 50%, and (C) 68%. APCDI, atmospheric pressure corona discharge ionization.

electron is localized on such unstable ions or on the polar molecules. Therefore, here we suppose that the anion at *m/z* 20 is produced as a dipole-bound complex between hydrogen H_2, water H_2O, and electron e^-.

3.3. The formation of dipole-bound complex ion at *m/z* 22 by supplying HF

To elucidate the proposed ionic composition of the ion H_4O^- at *m/z* 20, here we performed the experiments with adding another polar molecule HF in expectation of the formation of H_3F^- ion at *m/z* 22. The negative ion APCDI mass spectra were obtained with supplying HF gas under several conditions. Here we used an HF generator[10] and used another method for generating HF molecules, *i.e.*, by supplying the vapor of a calibrant reagent PFK, because it is expected that hydrogen radicals generated by dissociation of water molecules on the tip of corona needle extract fluorine from PFK molecules. Figure 6 shows negative-ion APCDI mass spectra of ambient air obtained with supplying HF gas or the vapor of PFK molecules. It is noteworthy, as expected, that the spectra showed the ions at *m/z* 22 and its water clusters that may be assigned as $H_3F^-(H_2O)_n$ (n = 1–4) at *m/z* 40, 58, 76, and 94. The spectra showed other ions at *m/z* 19 originating from F^-, the hydroxide HO^-, and its water clusters $HO^-(H_2O)_n$ (n = 1–4) at *m/z* 17, 35, 53, 71, and 89, and the H_4O^- and its water cluster ions $H_4O^-(H_2O)_n$ (n = 1–3) at *m/z* 20, 38, 56, and 74. As already described above, high humidity and high electric field conditions gave the negative

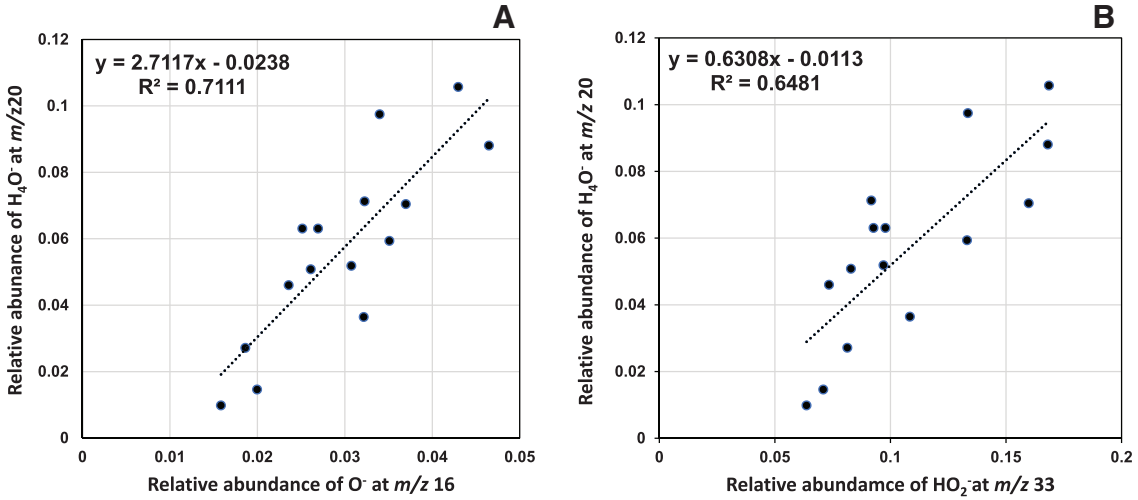

Fig. 3. Correlations for the formation of the ion at *m/z* 20 with the ions of (A) O^- at *m/z* 16 and (B) HO_2^- at *m/z* 33.

Table 1. Relative abundances for the ions at *m/z* 20 (H_4O^-), 16 (O^-), and 33 (HO_2^-) recorded in mass spectra obtained with the needle voltage of −2.0 to −3.4 kV.

Voltage (−kV)	*m/z* 20 H_4O^-	*m/z* 16 O^-	*m/z* 33 HO_2^-
2.0	0.00983	0.01584	0.06371
2.1	0.01461	0.01997	0.07096
2.2	0.02714	0.01863	0.08135
2.3	0.03645	0.03217	0.10844
2.4	0.05937	0.03510	0.13313
2.5	0.07044	0.03698	0.15986
2.6	0.08807	0.04649	0.16809
2.7	0.10572	0.04297	0.16862
2.8	0.09747	0.03398	0.13351
2.9	0.07126	0.03227	0.09174
3.0	0.06305	0.02695	0.09268
3.1	0.06306	0.02515	0.09783
3.2	0.05185	0.03076	0.09702
3.3	0.05082	0.02610	0.08291
3.4	0.04602	0.02358	0.07341

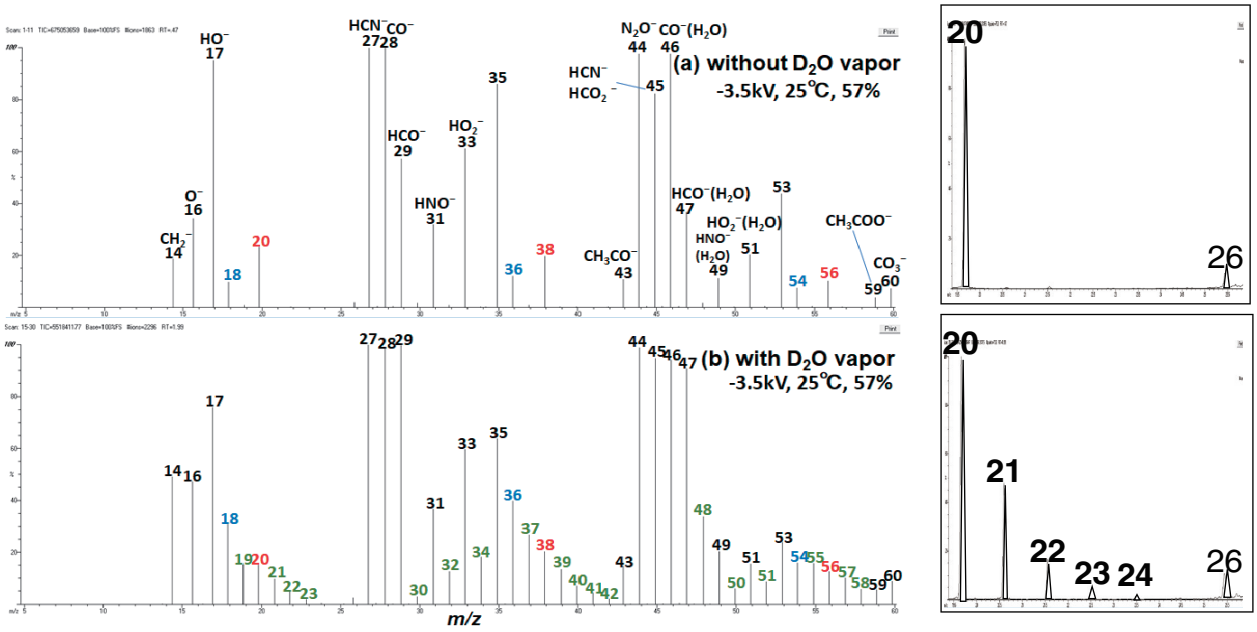

Fig. 4. Negative-ion APCDI mass spectra of ambient air obtained by supplying the vapor of D_2O. The right-hand insets indicate enlarged spectra at *m/z* 20. APCDI, atmospheric pressure corona discharge ionization.

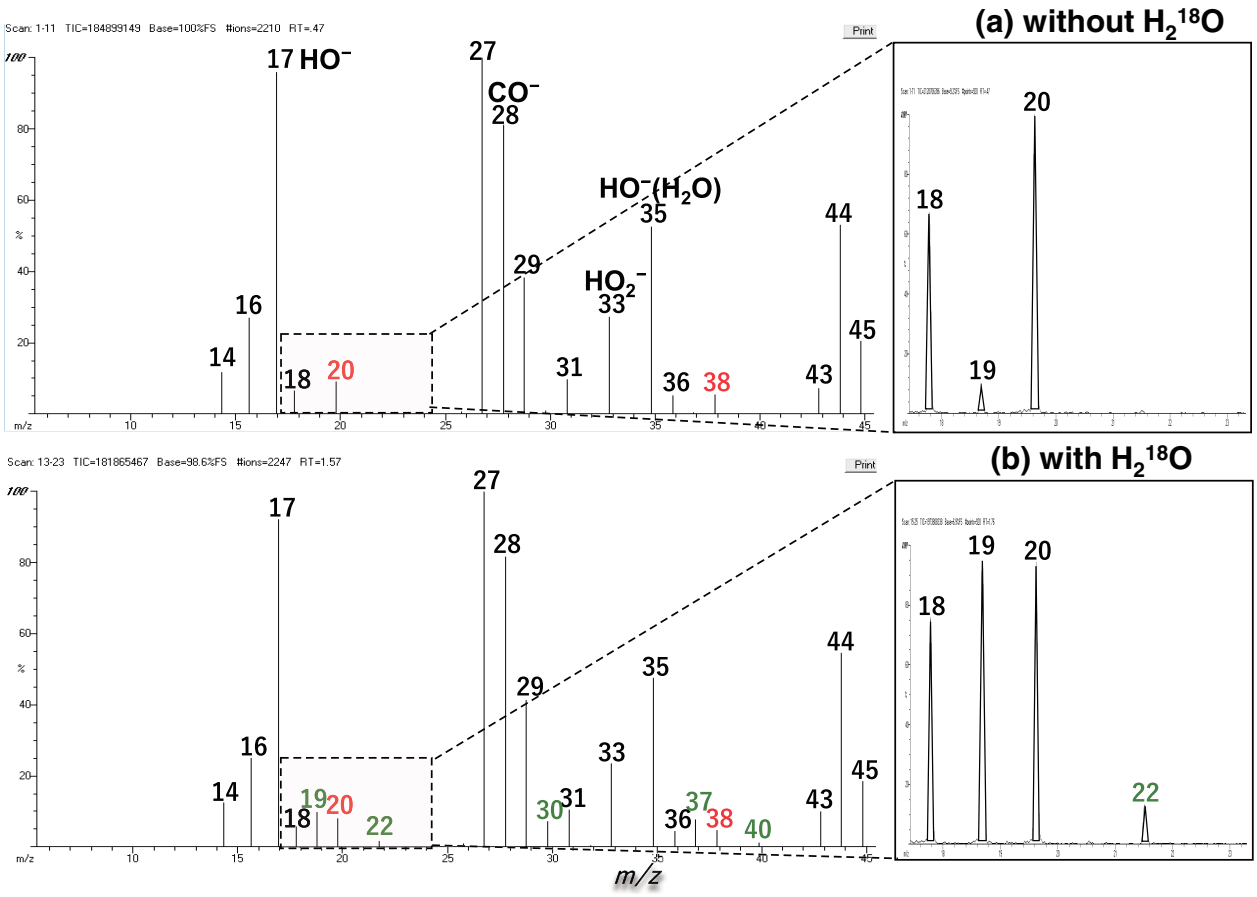

Fig. 5. Negative-ion APCDI mass spectra of ambient air obtained (a) without and (b) with $H_2{}^{18}O$. APCDI, atmospheric pressure corona discharge ionization.

ion at *m/z* 20, as shown in Fig. 6A and 6B, indicating that direct supply of the vapor of PFK seems to be more favorable for the formation of the ion at *m/z* 22 than the use of the HF generator. The high electric field combined with low humidity gave better conditions for the formation of the ion at *m/z* 22, although the ions at *m/z* 19 and 20 were slightly observed in Fig. 6C.

The definite observation of the unusual ionic species H_4O^- and H_3F^- implies that unstable or metastable H_2^- ion might be stabilized by the dipole-bound complexing with polar molecules such as H_2O and HF, as was theoretically proposed by the Skurski and Simons group.[9,16,19] Although the detailed processes for the formation of H_4O^- and H_3F^- ions are unclear at present, those ions may be formed by the ion–molecule reactions of H_2O, HF, H, H^-, and/or electrons under ambient conditions.

3.4. Stability and structure of the ions H_4O^- and H_3F^-

Next we calculate the stability and structure of the ions of H_4O^- and H_3F^- by using density functional theory (DFT) calculations to elucidate the ionic chemical compositions. The calculations for H_4O^- and H_3F^- could be successfully converged and gave appropriate ionic structures. The ionic structures and highest occupied molecular orbitals (HOMOs) of the complex ions of H_4O^- and H_3F^- are shown in Fig. 7. The Mulliken charge and spin density of the H_4O^- ion indicate that negative charge and attached electron (spin) are localized on the oxygen atom (O1) of the H_2O molecule, although the tail-end hydrogen (H5) of the H_2 molecule has slightly negative charge (Table 2). In case of the H_3F^- ion, the negative charge is distributed on the fluorine (F1) of HF and the tail-end hydrogen (H4) of H_2, while the attached electron (spin) is merely localized on the fluorine (F1) of the HF molecule (Table 3). The results calculated above indicate that the ions of H_4O^- and H_3F^- have non-covalent bonding ionic structures or the dipole-bound complex structures of $H_2O^-\cdots H_2$ (or $H_2O\cdots H_2^-$) and $HF^-\cdots H_2$ (or $HF\cdots H_2^-$), respectively. From the calculated results, it is suggested that the ions of H_4O^- and H_3F^- are formed by the interaction of neutral molecule of H_2O or HF with H_2 and electron, and that electron is delocalized on the complex ($H_2O\cdots H_2$) or ($HF\cdots H_2$).

To estimate the stability of the dipole-bound complex ions described above, the free energy changes ΔG for the reactions of $(H_2 + H_2O)^- \rightarrow (H_2O^-\cdots H_2)$ or $(H_2O\cdots H_2^-)$ and $(H_2 + HF)^- \rightarrow (HF^-\cdots H_2)$ or $(HF\cdots H_2^-)$ were calculated using the same functional level of theory and basis set. The results obtained are summarized in Table 4. The complexing reactions of neutral hydrogen H_2 with negative ions of H_2O^- and HF^- showed slightly negative values of ΔG, which mean exothermic, while the reactions of negative hydrogen H_2^- with neutral molecules were largely endothermic. The exothermic reactions of neutral hydrogen with negative polar molecules indicate that the dipole-bound complex states of $H_2O^-\cdots H_2$ and $HF^-\cdots H_2$ are thermodynamically stable and consistent with the calculated ionic structures shown in Fig. 7.

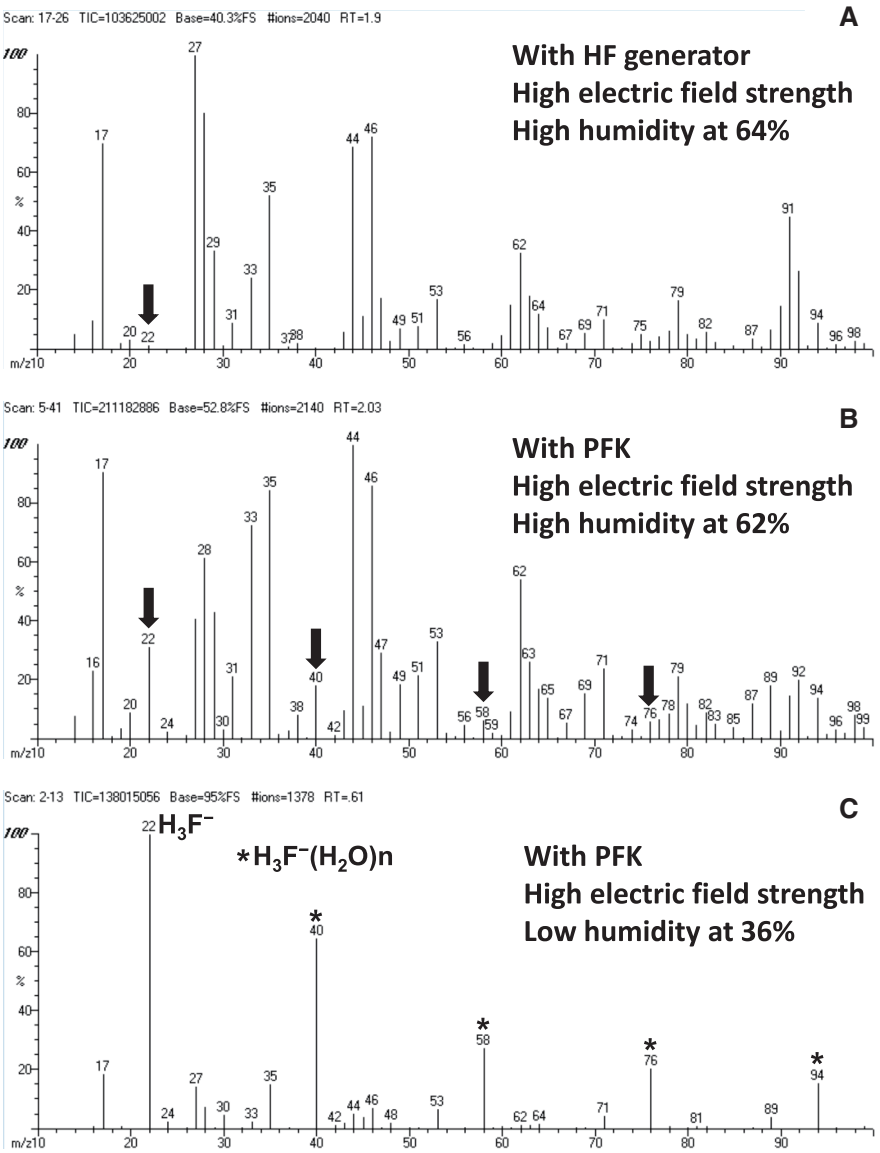

Fig. 6. Negative-ion APCDI mass spectra of ambient air obtained with high electric field strength under the conditions of (A) HF gas at 64% humidity, (B) PFK at 62% in humidity, and (C) PFK at 36% humidity. APCDI, atmospheric pressure corona discharge ionization; HF, hydrogen fluoride; PFK, perfluorokerocene.

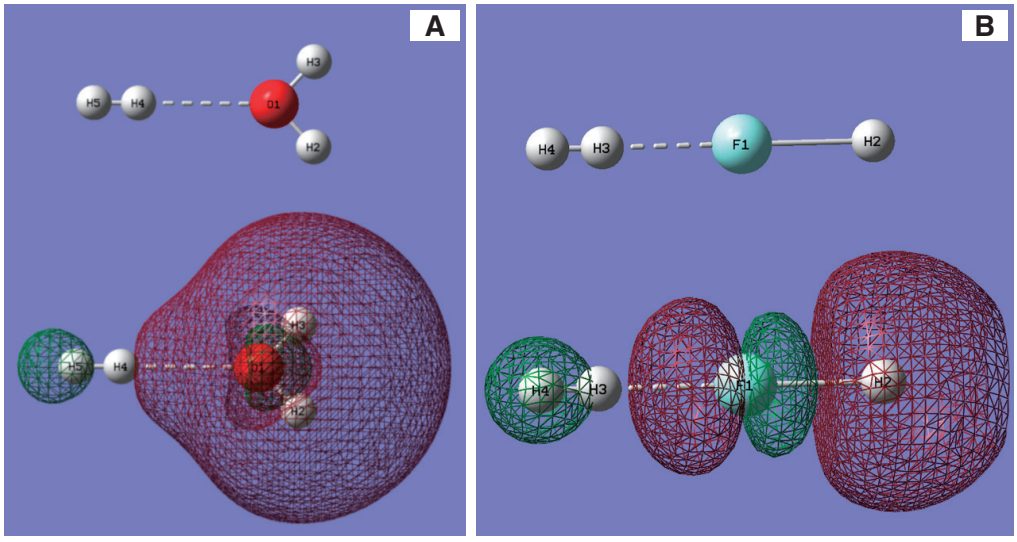

Fig. 7. Highest occupied molecular orbitals and dipole-bound complex structures of (A) $H_2…OH_2$ and (B) $H_2…FH$ obtained by DFT calculations for H_4O^- and H_3F^-. DFT, density functional theory.

Table 2. Mulliken charges 1 and spin densities 2 of H_4O^-.

		1	2
1	O	−1.649629	1.017438
2	H	0.329641	−0.016132
3	H	0.329641	−0.016132
4	H	0.171328	0.005307
5	H	−0.180982	0.009519

Table 3. Mulliken charges 1 and spin densities 2 of H_3F^-.

		1	2
1	F	−1.515993	1.262231
2	H	0.591796	−0.310891
3	H	0.748428	0.035705
4	H	−0.824230	0.012955

Table 4. Free energy change ΔG of the reactions for complexing of hydrogen with water and HF molecules.

Reaction	Free energy change (kJ/mol)
$H_2 + H_2O^- \rightarrow H_2O^-\ldots H_2$	−6.97
$H_2^- + H_2O \rightarrow H_2O\ldots H_2^-$	131.99
$H_2 + HF^- \rightarrow HF^-\ldots H_2$	−2.90
$H_2^- + HF \rightarrow HF\ldots H_2^-$	190.50

HF, hydrogen fluoride.

4. CONCLUSION

The negative-ion at *m/z* 20 produced by APCDI of ambient air was identified as the chemical composition of H_4O by supplying the vapor of D_2O and $H_2{}^{18}O$. The abundance of the ion at *m/z* 20 increased with increasing the humidity in ambient air at high electric field condition. The supply of HF gas or the vapor of PFK as a source of HF gas resulted in a negative ion at *m/z* 22, suggesting the formation of H_3F^-, whereby HF is complexing with H_2 and electron. The formation of the negative ions H_4O^- and H_3F^- was discussed from the viewpoint of the dipole-bound complex between electron e^-, hydrogen H_2, and polar molecules such as H_2O and HF having the dipole moment beyond the critical dipole moment, theoretically proposed by the Skurski and Simons group.[9,16,19] According to the proposition, the hydrogen anion H_2^- can be stabilized by complexing with the polar molecules such as H_2O and HF. However, it is difficult to say that the complex ions H_4O^- and H_3F^- have sufficient stability in air and even in the mass spectrometer, because the negative ions H_2^-, H_2O^-, and HF^- are metastable or unstable with short lifetimes in itself. The DFT calculations suggested that the ions H_4O^- and H_3F^- have the dipole-bound complex structures $H_2O^-\ldots H_2$ and $HF^-\ldots H_2$ and also that electrons are delocalized over the whole of the complex $H_2O\ldots H_2$ and $HF\ldots H_2$. It was shown, furthermore, by the DFT calculations that the ionic structures $H_2O^-\ldots H_2$ and $HF^-\ldots H_2$ are produced by exothermic reactions, while the formation of the ions involving negative hydrogen, $H_2O\ldots H_2^-$, and $HF\ldots H_2^-$, is produced by endothermic reactions.

REFERENCES

1) K. Nagato, Y. Matsui, T. Miyata, T. Yamauchi. An analysis of the evolution of negative ions produced by a corona ionizer in air. *Int. J. Mass Spectrom*. 248: 142–147, 2006.
2) K. Sekimoto, M. Takayama. Influence of needle voltage on the formation of negative core ions using atmospheric pressure corona discharge in air. *Int. J. Mass Spectrom*. 261: 38–44, 2007.
3) K. Sekimoto, M. Takayama. Dependence of negative ion formation on inhomogeneous electric field strength in atmospheric pressure negative corona discharge. *Eur. Phys. J. D* 50: 297–305, 2008.
4) K. Sekimoto, M. Takayama. Observations of different core water cluster ions $Y^-(H_2O)_n$ ($Y=O_2$, HO_x, NO_x, CO_x) and magic number in atmospheric pressure negative corona discharge mass spectrometry. *J. Mass Spectrom*. 46: 50–60, 2011.
5) F. C. Fehsenfeld, E. E. Ferguson. Laboratory studies of negative ion reactions with atmospheric trace constituents. *J. Chem. Phys*. 61: 3181–3193, 1974.
6) J. C. Rienstra-Kiracofe, G. S. Tschumper, H. F. Schaefer III, S. Nandi, B. Ellison. Atomic and molecular electron affinities: Photoelectron experiments and theoretical computations. *Chem. Rev*. 102: 231–282, 2002.
7) K. Sekimoto, M. Takayama. Negative ion formation and evolution in atmospheric pressure corona discharges between point-to-plane electrodes with arbitrary needle angle. *Eur. Phys. J. D* 60: 589–599, 2010.
8) H. Takahashi, Y. Shimabukuro, D. Asakawa, S. Yamauchi, S. Sekiya, S. Iwamoto, M. Wada, K. Tanaka. Structural analysis of phospholipid using hydrogen abstraction dissociation and oxygen attachment dissociation in tandem mass spectrometry. *Anal. Chem*. 90: 7230–7238, 2018.
9) P. Skurski, J. Simons. An unstable anion stabilized in a molecular trap. *J. Phys. Chem. A* 104: 712–717, 2000.
10) K. Sakamoto, K. Sekimoto, M. Takayama. Collision-induced dissociation study of strong hydrogen-bonded cluster ions $Y^-(HF)_n$ ($Y=F$, O_2) using atmospheric pressure corona discharge ionization mass spectrometry combined with a HF generator. *Mass Spectrom. (Tokyo)* 6: A0063, 2017.
11) M. J. Frisch, G. W. Trucks, H. B. Schlegel, G. E. Scuseria, M. A. Robb, J. R. Cheeseman, G. Scalmani, V. Barone, G. A. Petersson, H. Nakatsuji, X. Li, M. Caricato, A. V. Marenich, J. Bloino, B. G. Janesko, R. Gomperts, B. Mennucci, H. P. Hratchian, J. V. Ortiz, A. F. Izmaylov, J. L. Sonnenberg, D. Williams-Young, F. Ding, F. Lipparini, F. Egidi, J. Goings, B. Peng, A. Petrone, T. Henderson, D. Ranasinghe, V. G. Zakrzewski, J. Gao, N. Rega, G. Zheng, W. Liang, M. Hada, M. Ehara, K. Toyota, R. Fukuda, J. Hasegawa, M. Ishida, T. Nakajima, Y. Honda, O. Kitao, H. Nakai, T. Vreven, K. Throssell, J. A. Montgomery, Jr., J. E. Peralta, F. Ogliaro, M. J. Bearpark, J. J. Heyd, E. N. Brothers, K. N. Kudin, V. N. Staroverov, T. A. Keith, R. Kobayashi, J. Normand, K. Raghavachari, A. P. Rendell, J. C. Burant, S. S. Iyengar, J. Tomasi, M. Cossi, J. M. Millam, M. Klene, C. Adamo, R. Cammi, J. W. Ochterski, R. L. Martin, K. Morokuma, O. Farkas, J. B. Foresman, and D. J. Fox. *Gaussian 16, Revision C.01*. Gaussian, Inc., Wallingford CT, 2019.
12) Y. Zhao, D. G. Truhlar. The M06 suite of density functionals for main group thermochemistry, thermochemical kinetics, noncovalent interactions, excited states, and transition elements: Two new functionals and systematic testing of four M06-class functionals and 12 other functionals. *Theor. Chem. Acc*. 120: 215–241, 2008.
13) J. S. Chang, R. M. Hobson, Y. Ichikawa, T. Kaneda. Denri Kitai no Genshi·Bunshi Katei (in Japanese), Tokyo Denki Daigaku Shuppan-kyoku, Tokyo, 1982, p. 107.
14) R. E. Ballard. The electron affinity of water and the structure of the hydrated electron. *Chem. Phys. Lett*. 16: 300–301, 1972.
15) B. Jordon-Thaden, H. Kreckel, R. Golser, D. Schwalm, M. H. Berg, H. Buhr, H. Gnaser, M. Grieser, O. Heber, M. Lange, O. Novotný, S.

Novotny, H. B. Pedersen, A. Petrignani, R. Repnow, H. Rubinstein, D. Shafir, A. Wolf, D. Zajfman. Structure and stability of the negative hydrogen molecular ion. *Phys. Rev. Lett*. 107: 193003, 2011.

16) C. Desfrançois, H. Abdoul-Carime, N. Khelifa, J. P. Schermann. From $1/r$ to $1/r^2$ potentials: Electron exchange between Rydberg atoms and polar molecules. *Phys. Rev. Lett*. 73: 2436–2439, 1994.

17) J. Simons, K. D. Jordan. Ab initio electronic structure of anions. *Chem. Rev*. 87: 535–555, 1987.

18) https://cccbdb.nist.gov/diplistx.asp.

19) M. Sobczyk, I. Anusiewicz, P. Skurski. Shape resonance of H_2^- anion stabilized in a molecular trap. *J. Chem. Phys*. 118: 7297–7302, 2003.